Volume 12, Issue 1, December 2025 ISSN 2542-2545

The HIMALAYAN PHYSICS

A peer-reviewed Journal of Physics

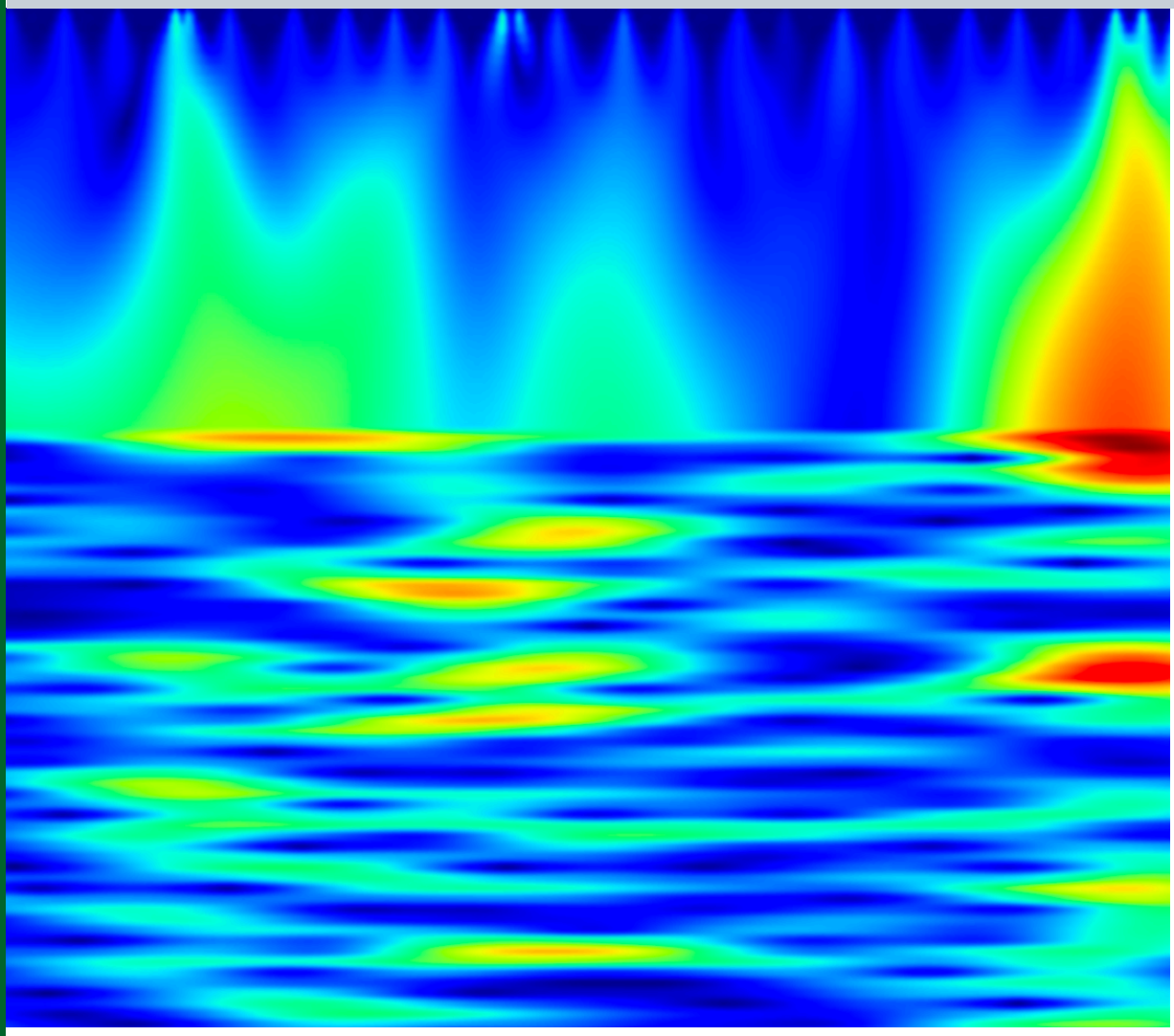

Department of Physics, Prithvi Narayan Campus, Pokhara
Nepal Physical Society, Gandaki Chapter, Pokhara

Publisher

Department of Physics, Prithvi Narayan Campus, Pokhara
Nepal Physical Society, Gandaki Chapter, Pokhara

The Himalayan Physics

Volume 12, Issue 1, December 2025

ISSN 2542-2545

The Himalayan Physics (HimPhys) is an open access peer-reviewed journal that publishes quality articles which make innovative contributions in all areas of Physics. HimPhys is published annually by Nepal Physical Society (Gandaki Chapter), and Department of Physics, Prithvi Narayan Campus, Pokhara. The goal of this journal is to bring together researchers and practitioners from academia in Nepal and abroad to focus on advanced techniques and explore new avenues in all areas of physical sciences and establishing new collaborations with physics community in Nepal.

Chief Editor

Aabiskar Bhusal

Cover: Wavelet time–frequency representation for the NEAR condition. The figure shows stronger low-frequency activity over time, suggesting greater mental effort and engagement when surrounding stimuli are close to the target. (Figure 3(a), Himalayan Physics 12, 1-14, (2025))

Volume 12, Issue 1, December 2025 ISSN 2542-2545

The HIMALAYAN PHYSICS

A peer-reviewed Journal of Physics

Publisher

Department of Physics, Prithvi Narayan Campus, Pokhara

Nepal Physical Society, Gandaki Chapter, Pokhara

Nepal Physical Society

Gandaki Chapter

Pokhara, Nepal

Himalayan Physics Vol-12(1) (2025)

TABLE OF CONTENTS

****

Him. Phys. **12** 83-100, (2025) ISSN: 2542-2545

Himalayan Physics

Exploration of structural, mechanical, dynamical, thermal, electronic, and magnetic properties of XFeSb (X = Nb, V, Ta) half-Heusler compounds: First-principles study

https://doi.org/10.3126/hp.v12i1.85760

Om Shree Rijal[1,2], Ganesh Paudel[1,2], Sukrit Kumar Yadav[1], Karan Deuba[1], Hari Krishna Neupane[1]*, Rajendra Parajuli[1]

1 Amrit Campus, Institute of Science and Technology, Tribhuvan University, Kathmandu, Nepal

2 These authors contributed equally.

Abstract: Half-Heusler (HH) compounds are promising candidates for thermoelectric, electronic, and energy-related applications. In the present work, we explored the structural, mechanical, dynamical, thermal, electronic, and magnetic properties of NbFeSb, VFeSb, and TaFeSb half-Heusler (HH) compounds using DFT methods through VASP software. For the structural properties, we calculated the ground-state energy and the bond lengths between nearest-neighbor atoms in the materials. We found that the studied compounds are structurally stable. The mechanical properties of the materials are examined through the calculations of their elastic constants and modulus of rigidity. It is found that NbFeSb, VFeSb, and TaFeSb are mechanically stable. Based on the calculated values of modulus of rigidity and anisotropic index, all the compounds exhibit hardness and anisotropic properties. Based on Pugh's and Poisson's ratios, NbFeSb and TaFeSb have ductile properties, whereas VFeSb exhibits a brittle nature. The dynamical properties of the materials are examined through their phonon dispersion curves and are found to be dynamically stable. Moreover, we have determined the phonon velocities and Debye temperature of the considered compounds and found that NbFeSb, VFeSb, and TaFeSb exhibit good thermal properties. The electronic properties of NbFeSb, VFeSb, and TaFeSb are explored through the analysis of their band structures and DOS plots; they are found to be small band-gap semiconducting materials. The magnetic properties of the materials are calculated by analyzing their DOS and PDOS plots and are found to be non-magnetic materials.

Keywords: Half Heusler Compounds • Phonon • DOS • Band

Received: 2025-11-03 **Revised: 2025-12-15** **Published: 2025-12-20**

I. Introduction

The half-Heusler (HH) materials have attracted significant attention in recent years due to their promising properties [1, 2]. These materials find applications in diverse technological fields, including

* *Corresponding Author: hari.neupane@ac.tu.edu.np*

spintronic devices [3, 4], optoelectronics devices [5, 6], catalysis [7], thermoelectric materials [7, 8], magnetoelectronic materials [9], and superconductors [10]. NbFeSb is a half-Heusler intermetallic compound that has recently attracted considerable interest as a promising thermoelectric material. This interest arises from its environmentally friendly characteristics and the relatively high natural abundance of Nb and Fe. Half-Heusler XMZ materials are considered a key foundation for many modern technological applications. They are widely utilized in fields such as renewable energy, spintronics, and other related advanced technologies. Half-Heusler (HH) compounds are versatile semiconducting materials. They have strong mechanical stability and can withstand high temperatures. These materials show high zT values and good thermoelectric performance. As a result, they are suitable for applications such as solar cells, transparent conductors, piezoelectric devices, and spintronics [3, 4]. HH material has a standard composition of XYZ elements in a stoichiometric ratio (1 : 1 : 1), where X is an early transition metal such as (Sc, Ti), Y is a late transition metal such as (Fe, Co, Ni), and Z is a heavy main group metal (Sn, Sb, *or* Pb) [11]. Additionally, X and Y atoms exhibit a clear cationic nature, while Z can be regarded as their anionic counterpart [12]. The HH structure can be described as a combination of zinc blende (YZ) and rock-salt (XZ) structures, belonging to the cubic space group $F\bar{4}3m$ (216), with X at 4a$(0, 0, 0)$, Y at 4c$(1/4, 1/4, 1/4)$, and Z at 4 b$(1/2, 1/2, 1/2)$ [13]. Each element possesses either a full or empty shell, and a balanced oxidation state indicates a stable composition [14]. HH materials with a valence electron count (VEC) of 18 are typically non-magnetic and exhibit a closed-shell structure [15–17], whereas those with a VEC of 19 or 22 display half-metallic behavior, making them suitable for spintronic devices [18, 19].

Nakajima et al. in 2015 [20] studied the physical properties of RPdBi HH compound through density functional theory (DFT) method, and found that it exhibits superconducting and magnetic properties. Li and co-authors in 2016 [1] reported the effect of substituting Hf or Zr in the TiNiSn HH compound, and determined its mechanical strength. Eliassen et al. in 2017 [21] studied lattice thermal conductivity in Ti-based HH materials based on their thermal stability and electronic properties, and found that they are thermally stable and are favorable for thermoelectric devices. However, these compounds also present several challenges that limit their overall effectiveness. HH materials have fewer atoms per unit cell and have a highly symmetric structure, which leads to higher thermal conductivity [21, 22]. For both p-type and n-type HH materials, the maximum calculated values are close to unity [23, 24]. HH compounds have attracted significant interest due to their multifunctional electronic, magnetic, thermal, and transport properties. Early studies reported superconductivity and magnetism in RPdBi [20] and improved mechanical strength in TiNiSn through Hf or Zr substitution [1]. In 2020, Mohamed tuned the physical properties of NbFeSb by doping / co-doping Co atoms in the structure [23]. Later, authors have examined the structural, electronic, magnetic, and thermal properties of various HH compounds by the effect of defects and doping on the compounds [24–26].

We have reviewed the existing literature on half-Heusler (HH) compounds and identified that the

structural, mechanical, dynamical, thermal, electronic, and magnetic properties of NbFeSb, VFeSb, and TaFeSb remain relatively unexplored. These gaps represent unresolved issues and constitute the research gap between previous studies and the present work. Therefore, our motivation is to investigate the structural, mechanical, dynamical, thermal, electronic, and magnetic properties of NbFeSb, VFeSb, and TaFeSb HH compounds using a DFT approach with VASP computational tools.

II. Methods and Materials

We study the structural, electronic, magnetic, mechanical, and optical properties of the XFeSb(X = Nb, V, Ta) half-Heusler (HH) compounds using the density functional theory (DFT) method [27] through the Vienna *ab* initio Simulation Package (VASP) [28] as a computational tool. The Perdew-Burke-Ernzerhof (PBE) [29] exchange-correlation functional, along with the projector augmented wave (PAW) pseudopotential, is used to handle the interactions between the valence electrons of atoms in the materials, where the valence-electron configurations of the constituent atoms are Nb $= 4d^4, 5s^1$, Ta $= 5d^3, 5s^1$, V $= 3d^3, 4s^2$, Fe $= 3d^3, 4s^2$, and Sb $= 5s^2, 5p^3$. Structural optimizations were performed using a kinetic energy cutoff of 520 eV, which was determined from convergence tests for the cutoff energy. In addition, Brillouin zone integrations within the plane-wave method employed an $8 \times 8 \times 8$ k-point mesh, which was also obtained from convergence tests for the k-point sampling in the first irreducible Brillouin zone (BZ). Then, after relaxation calculations are done using the Hellmann-Feynman method [30] until the forces on each atom reach below 0.01 eV/Å, hence, optimized and relaxed structures of NbFeSb, VFeSb, and TaFeSb HH compounds are obtained. The electronic and magnetic properties of NbFeSb, VFeSb, and TaFeSb HH are predicted through the analysis of their band structure, density of states (DOS) plots, and DOS and partial DOS (PDOS) plots. For the band structure, we used a $(12 \times 12 \times 12)$ k-point mesh in the irreducible Brillouin zone (BZ), while a $(24 \times 24 \times 24)$ k-point mesh is used for DOS and PDOS calculations, as a denser mesh of k-points produces smoother DOS/PDOS states. The dynamical properties of NbFeSb, VFeSb, and TaFeSb HH compounds are evaluated using the density functional perturbation theory (DFPT) methods using a $2 \times 2 \times 2$ q-point mesh. Examining the phonon dispersion offers valuable insight into thermal transport properties and helps assess the dynamical stability of the compound [31]. Furthermore, the mechanical properties of materials are investigated by analyzing their elastic constants and modulus of rigidity through Voigt-Reuss-Hill (VRH) approximation [32–34].

III. Results and Discussion

In this section, we provide a detailed interpretation of this work.

Structural Properties

Structural properties are fundamental characteristics that define the atomic arrangement and crystallographic structure of a material. They include lattice parameters, atomic positions, and interatomic distances of atoms in the structure. Precisely determining these properties is crucial for understanding the material's stability, bonding characteristics, and their impact on its physical and chemical behavior. In the present work, we have determined the structural parameters of NbFeSb, VFeSb, and TaFeSb HH compounds by the DFT method. The optimized and relaxed structures of NbFeSb, VFeSb, and TaFeSb HH compounds are shown in Fig. 1. The structures of NbFeSb, VFeSb, and TaFeSb are cubic [35].

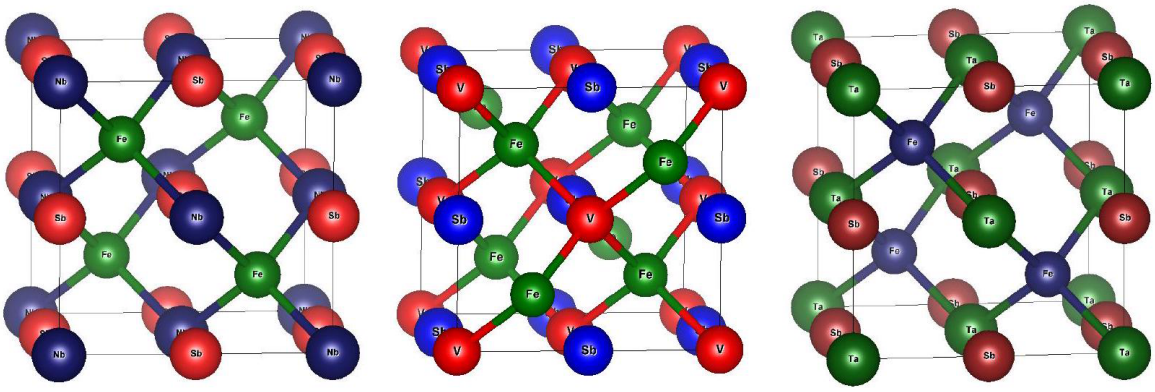

Figure 1. Optimized and relaxed structures of HH compounds: (a) NbFeSb, (b) VFeSb, and (c) TaFeSb

The Wyckoff positions of (X = Nb, V, Ta), Sb, and Fe atoms in the considered structures are 4a(0, 0, 0), 4 b(1/2, 1/2, 1/2), and 4 d(1/4, 1/4, 1/4), respectively. For the structure analysis, we calculated the bond length between the two nearest atoms in the structures. The calculated bond lengths between Nb − Fe, Fe − Sb, and Nb − Sb atoms in the NbFeSb compound are found to be 2.64 Å, 2.64 Å, and 3.05 Å; those between V-Fe, Fe-Sb, and V-Sb atoms in the VFeSb compound are 2.58 Å, 2.58 Å, and 2.97 Å; and between Ta − Fe, Fe − Sb, and Ta − Sb atoms in the TaFeSb compound are 2.59 Å, 2.59 Å, and 2.99 Å, respectively. These values are in good agreement with the previously reported bond lengths in the TiNiSn material [36]. The calculated lattice parameters of NbFeSb, VFeSb, and TaFeSb HH compounds are 6.09 Å, 5.94 Å, and 5.99 Å, respectively. They are in agreement with the reported works of other HH compounds [37, 38]. Additionally, we have also calculated the total formation energy (sum of internal energy of the system) to examine the stability of NbFeSb, VFeSb, and TaFeSb HH compounds by using equation (1),

$$E_{\text{for}} = \frac{E_{xyz} - (xE_x + yE_y + zE_z)}{x + y + z}, \tag{1}$$

where E_{for} is the formation energy, E_{xyz} is the total energy of the compound, and E_x, E_y, E_z are the energies per atom of the x, y, and z constituent atoms, respectively. Materials with higher (more negative)

total energy values are more stable in the system. In our case, the calculated value of formation energy is found to be -66.93 eV for NbFeSb, -56.31 eV for VFeSb, and -67.13 eV for TaFeSb, respectively. These minimum values of ground state energy of materials imply that they are stable compounds. Therefore, from the analysis of the structure parameters of materials, we found that our considered HH compounds are structurally stable. The calculated values of bond lengths of considered materials are presented in Table 1 which are in close agreement with the reported values [36].

Table 1. Calculated bond lengths of NbFeSb, VFeSb, and TaFeSb HH compounds, and reported bond lengths of other HH compounds.

HH Compounds	Calculated values of bond length ($\AA$)	Reported values of bond length ($\AA$)
NbFeSb	Nb-Fe $= 2.64, \text{Fe} - \text{Sb} = 2.64, \text{Nb} - \text{Sb} = 3.05$	2.57, 2.97[36]
VFeSb	$\text{V} - \text{Fe} = 2.58, \text{Fe} - \text{Sb} = 2.58,\ \text{V} - \text{Sb} = 2.97$	-
TaFeSb	$\text{Ta} - \text{Fe} = 2.59, \text{Fe} - \text{Sb} = 2.59, \text{Ta} - \text{Sb} = 2.99$	-

Mechanical Properties

Mechanical properties of materials define their behavior under applied forces, loads, and varying environmental conditions, which in turn determine their suitability for engineering and industrial applications. These characteristics govern a material's strength, deformation response, and overall durability. In the present work, we discussed the material's stability, hardness, ductility or brittleness, and isotropic or anisotropic nature based on their elastic constants and modulus of rigidity. For these, we have calculated elastic constants (C_{ij} where $C_{ij} = C_{11}, C_{12}, C_{44}$), Bulk modulus ($B$), Shear modulus ($G$), Young's modulus (($Y$)), anisotropic factor ($A$), Pugh's ratio ($B/G$), and Poisson's ratio ($\nu$) of NbFeSb, VFeSb, and TaFeSb HH compounds using Voigt-Reuss-Hill approximations (VRH) [39–41]. Mechanical stability of the considered compounds is determined through the Born and Huang stability criteria, which are given by the following relations [42]:

$$C_{11} > 0, \tag{2}$$

$$C_{44} > 0, \tag{3}$$

$$C_{11} - C_{12} > 0, \tag{4}$$

$$C_{11} + 2C_{12} > 0, \tag{5}$$

NbFeSb, VFeSb, and TaFeSb HH compounds satisfy the stability criteria and are found to be mechanically stable materials. B, G, and Y of materials are determined by equations (6), (8), and (11), respectively:

$$B = \frac{B_V + B_R}{2}, \tag{6}$$

where B_V and B_R are the Voigt and Reuss bulk moduli, given by

$$B_V = B_R = \frac{C_{11} + 2C_{12}}{3}, \tag{7}$$

$$G = \frac{G_V + G_R}{2},, \tag{8}$$

where G_V and G_R are the Voigt and Reuss shear moduli, given by

$$G_V = \frac{C_{11} - C_{12} + 3C_{44}}{5} \tag{9}$$

$$G_R = \frac{5\,(C_{11} - C_{12})}{3\,(C_{11} - C_{12} + 4C_{44})} \tag{10}$$

$$Y = \frac{9BG}{3B + G} \tag{11}$$

From the calculations, the values of B, G, and Y are found to be high. A higher modulus of rigidity indicates that the material possesses greater hardness, meaning more force is required to deform its shape. The isotropic or anisotropic nature of materials is determined through their anisotropic factor (A), which is given by equation (12):

$$A = \frac{2C_{44}}{C_{11} - C_{12}} \tag{12}$$

The material exhibits isotropic behavior when A equals one; otherwise, it is anisotropic. The A values for NbFeSb, VFeSb, and TaFeSb are $0.04, 0.06$, and 1.08 , respectively. Since these values deviate from unity, materials are considered anisotropic. Material ductility and brittleness are examined through the calculations of their Pugh's ratio (B/G) and Poisson's ratio. A material has brittle properties if its Pugh's ratio is less than 1.75 ; otherwise, the material has ductile properties [43]. Pugh's ratio of NbFeSb, TaFeSb, and VFeSb are found to be 2.30, 4.72, and 1.45, respectively. It means NbFeSb and TaFeSb have ductile properties, whereas VFeSb has a brittle nature. Poisson's ratio (ν) of materials also predicts the materials' ductility and brittleness, which is obtained using equation (13):

$$\nu = \frac{2B - 3G}{2(3B + G)} \tag{13}$$

If the value of ν is less than 0.26 , materials will have a brittle nature; otherwise, they have a ductile nature [44]. The ν of NbFeSb, TaFeSb, and VFeSb are found to be $0.31, 0.40$, and 0.22 , respectively. They reflect that VFeSb has brittle properties, whereas NbFeSb and TaFeSb have ductile properties. Materials' ductile and brittle nature is predicted by the analysis of their Pugh's and Poisson's ratio. The calculated parameters for the prediction of the material's mechanical properties are presented in Table 2.

Table 2. Calculated values of elastic constants (C_{11}, C_{12}, C_{44}), Young's modulus (Y), Bulk modulus (B), Shear modulus (G), Pugh's ratio (B/G), Anisotropic factor (A), and Poisson's ratio ν of NbFeSb, TaFeSb, and VFeSb HH compounds.

Calculated Parameters	NbFeSb	VFeSb	TaFeSb
C_{11} (GPa)	277.91	282.12	418.05
C_{12} (GPa)	101.33	65.66	213.34
C_{44} (GPa)	59.41	86.34	40.87
Bulk modulus B (GPa)	160.20	137.81	281.57
Shear modulus G (GPa)	69.66	94.51	59.63
Pugh's ratio B/G	2.30	1.45	4.72
Young's modulus Y (GPa)	182.52	230.79	167.10
Anisotropic factor A	0.67	0.79	0.39
Poisson's ratio ν	0.31	0.22	0.40

Dynamical Properties

Dynamical properties of materials describe how the atoms or crystal lattice react to vibrations, external forces, or time-dependent perturbations. They are closely associated with atomic motion, phonon behavior, and the material's stability under dynamic conditions [45]. The dynamical (vibrational) stability of a material is predicted based on its phonon spectrum. A material is considered dynamically stable if all its phonon frequencies are positive; otherwise, it is dynamically unstable [46–48]. The phonon spectra (dispersion curve) of NbFeSb, VFeSb, and TaFeSb HH compounds are illustrated in Fig. 2. The phonon

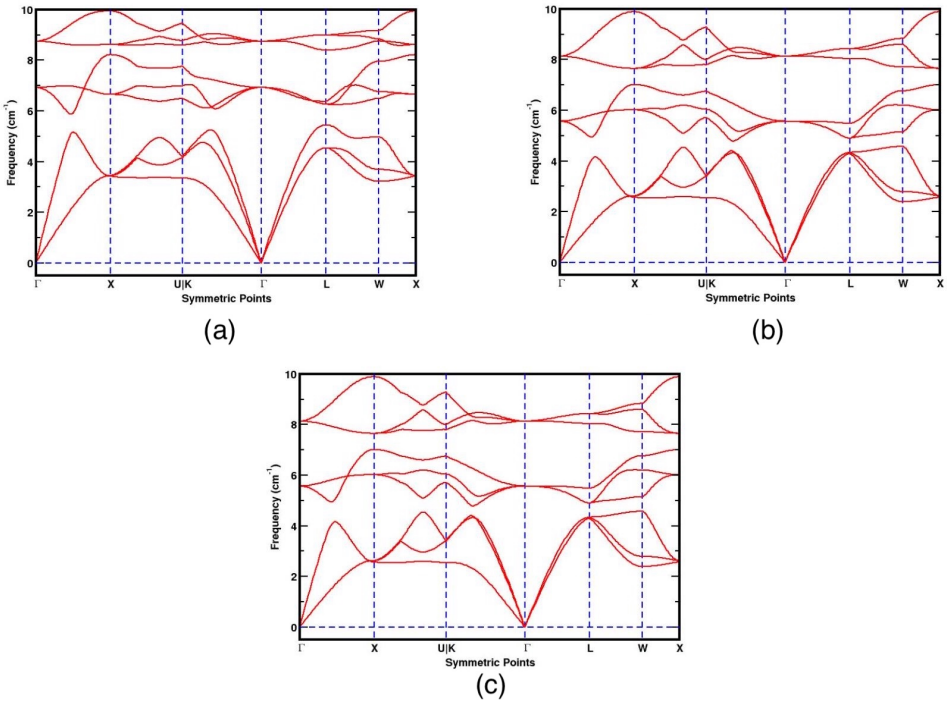

Figure 2. Phonon dispersion curves of: (a) NbFeSb HH compound, (b) VFeSb HH compound, and (c) TaFeSb HH compound. Highly symmetric points are taken along the x -axis, and phonon frequencies are taken along the y -axis.

dispersion curve of NbFeSb, TaFeSb, and VFeSb materials is studied in two different regions. They are called the lower frequency region (LFR) and the higher frequency region (HFR). The LFR corresponds to the acoustic modes, while the HFR corresponds to optical modes. The LFR for NbFeSb, TaFeSb, and VFeSb are elongating from (0.00 to 5.44) cm^{-1}, (0.00 to 4.56)cm^{-1}, and (0.00 to 4.57) cm^{-1}, respectively, whereas the HFR regions for the same compounds are extending from (5.85 to 9.93) cm^{-1}, (4.76 to 9.89) cm^{-1}, and (4.77 to 9.90) cm^{-1} respectively. The small band gap between LFR and HFR is due to the small mass differences of the atoms in the unit cell of the materials. In Fig. 2, nine vibrational modes are observed due to the presence of three atoms in each unit cell of HH compounds. Among these modes, the first three are called acoustic modes, which correspond to zero frequency at the gamma point, while the remaining modes are called optical modes. All the acoustic and optical modes have positive frequencies, which ensures that NbFeSb, TaFeSb, and VFeSb are dynamically stable compounds.

Our calculated phonon dispersion curves are in good agreement with previously reported results for this compound [49].

Thermal Properties

Atomic vibrations in solid materials can be described in terms of their Debye temperature (Θ_D) and phonon velocities, including the longitudinal phonon velocity (v_l), transverse phonon velocity (v_t), and the average phonon velocity (v_a). The thermal properties of materials are largely determined by these atomic vibrations. The Debye temperature is directly related to the phonon velocities, meaning that Θ_D corresponds to the highest vibrational (phonon) frequency in a crystal, while the phonon velocity represents the speed at which lattice vibrations propagate through the material [50–53]. Furthermore, the Debye temperature of a material is associated with the average phonon velocity, which can be expressed using the following equations [54]:

$$\Theta_D = \frac{h}{k_B}\left(\frac{3N}{4\pi V}\right)^{1/3} v_m \tag{14}$$

$$v_m = \left[\frac{1}{3}\left(\frac{2}{v_t^3} + \frac{1}{v_l^3}\right)\right]^{-1/3} \tag{15}$$

where longitudinal and transverse velocities are given by

$$v_t = \sqrt{\frac{G}{\rho}}, \tag{16}$$

$$v_l = \sqrt{\frac{3B + 4G}{3\rho}}. \tag{17}$$

The calculated values of Debye temperature, phonon velocities, and melting point temperature (T_m) for NbFeSb, TaFeSb, and VFeSb are given in Table 3.

Table 3. Calculated values of Debye temperature (Θ_D), longitudinal velocity of phonon wave (v_l), transverse velocity of phonon wave (v_t), average velocity of phonon wave (v_a), and melting point temperature (T_m) for NbFeSb, TaFeSb, and VFeSb HH compounds.

Parameters	NbFeSb	VFeSb	TaFeSb
v_t(m/s)	2960.49	3619.51	2322.44
v_l(m/s)	5642.84	6047.33	5714.84
v_a(m/s)	3311.07	4005.01	2629.44
Θ_D(K)	370.50	459.00	299.00
T_m(K)	1973.12 ± 300	1994.63 ± 300	2689.23 ± 300

In Table 3, it is seen that the phonon velocities of the considered materials are higher. This means the materials have stronger interatomic bonding, higher stiffness, and better thermal conductivity. The Debye temperature of the considered materials is found to be higher because the Debye temperature is directly proportional to the average phonon velocity. The higher the value of the Debye temperature of materials implies that the stronger their interatomic bonding, the higher their melting point, and the higher their vibration frequency. Hence, NbFeSb, TaFeSb, and VFeSb have good thermal properties.

An empirical formula used to estimate the melting point of crystalline solids from their elastic constants is calculated by equation (18) [55]:

$$T_m = 553 + 5.11C_{11} \pm 300 \tag{18}$$

where ± 300 represents the possible uncertainty or range of prediction due to material-specific variation. The computed melting point temperatures of NbFeSb, VFeSb, and TaFeSb are 1973.12 ± 300 K, 1994.63 ± 300 K, and 2689.23 ± 300 K, respectively. These higher melting point temperatures reveal that the materials possess strong interatomic bonding, high phonon frequencies, and have high thermal stability. Therefore, NbFeSb, VFeSb, and TaFeSb HH compounds have good thermal properties and can be used in the fields of thermoelectric devices.

Electronic Properties

The electronic properties of materials refer to how they respond to an applied electric field, primarily determined by the arrangement and motion of electrons [56]. These properties are controlled by the material's band structure and density of states (DOS), which specify the permissible energy levels and the number of available states at each energy. Based on the band gap and DOS at the Fermi level, materials are categorized as metals, semiconductors, or insulators. Metals exhibit overlapping bands with a high DOS, semiconductors possess a small band gap, and insulators have a large band gap with zero DOS [57–59]. These characteristics collectively influence conductivity, carrier concentration, mobility, optical transitions, and overall electrical performance [60]. In the present work, we obtained the band structures and DOS plots of NbFeSb, VFeSb, and TaFeSb HH compounds, which are shown in Fig. 3.

In band plots, the highly symmetric points of materials in the irreducible Brillouin zone (BZ) are taken along the x -axis, and their corresponding energies are taken along the y -axis, whereas in DOS plots, band states are taken along the x -axis, and their corresponding energies are taken along the y -axis. In both plots, the horizontal dotted line represents the Fermi energy level, which distinguishes the valence band from the conduction band of the compounds. In NbFeSb, VFeSb, and TaFeSb, the valence band maximum (VBM) and the conduction band minimum (CBM) lie at distinct high-symmetry points from Γ to L , which indicates that the considered materials have indirect band gaps. The calculated band gap energies of NbFeSb, VFeSb, and TaFeSb are found to be 0.80 eV, 0.70 eV, and 0.73 eV , respectively. These calculated band gap energies are comparable with the band gap energies of reported works [37, 61]. Hence, NbFeSb, VFeSb, and TaFeSb are called small band gap semiconducting materials. Narrow band gap semiconducting materials can conduct more easily at room temperature, and are often used in thermoelectric, optoelectronic device applications [62, 63]. Therefore, NbFeSb, VFeSb, and TaFeSb can be used in the fields of optoelectronics, thermoelectrics, transistors, solar cells, and sensing applications. Additionally, we analyzed the DOS plots of the considered materials shown in Fig. 3 and observed that a

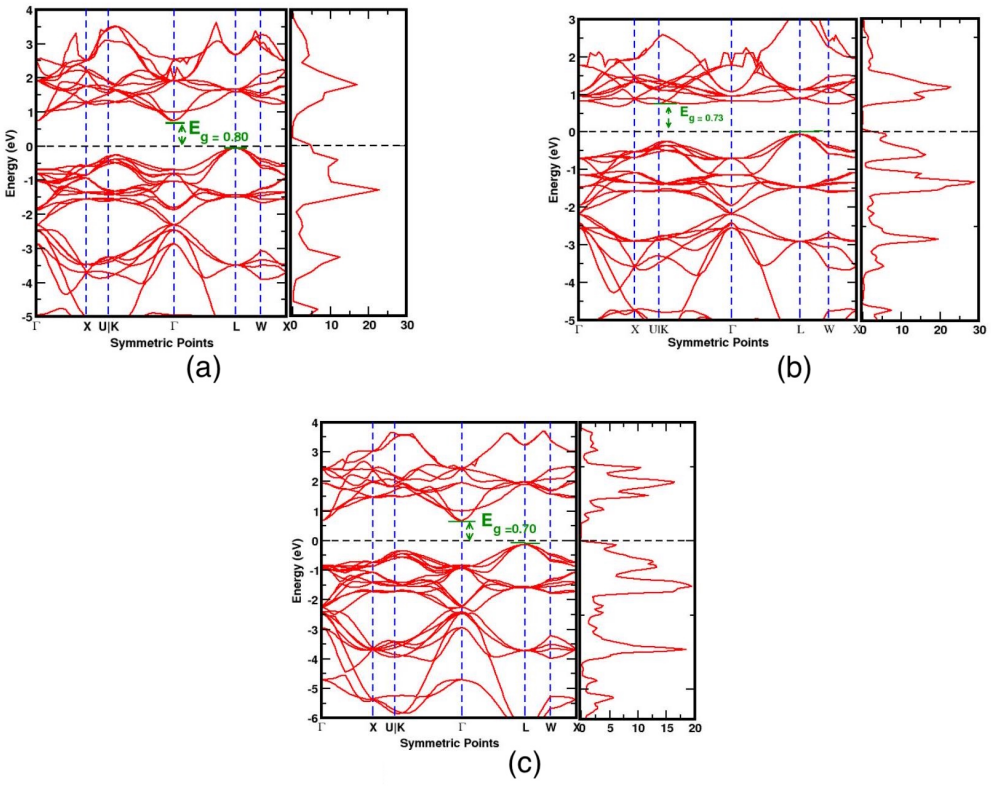

Figure 3. Band structures and density of states (DOS) plots of: (a) NbFeSb HH compound, (b) VFeSb HH compound, and (c) TaFeSb HH compound. The horizontal dotted line represents the Fermi energy level, and vertical dotted lines represent the highly symmetric points in the irreducible Brillouin zone.

zero value of DOS appeared at the Fermi energy level. Also, similar band gaps are indicated by the DOS

between the valence band and conduction band. Hence, this also confirms that our considered materials have small band gap energies.

Magnetic Properties

The magnetic and non-magnetic nature of materials is predicted by the analysis of their DOS and partial DOS (PDOS) plots [64]. The magnetic properties of materials are determined by analyzing the distribution of electronic spins around the Fermi energy level in DOS and PDOS plots. In magnetic materials, the spinup and spin-down DOS are unequal, and this difference in the number of spin-up and spin-down states near the Fermi energy level generates a net magnetic moment [65]. The spin-up and spin-down states of material are symmetrically distributed around the Fermi energy level; materials have non-magnetic properties, whereas spin-up and spin-down DOS are asymmetric, leading to finite magnetization [66]. Firstly, we analyzed the DOS plots of NbFeSb, VFeSb, and TaFeSb, HH compounds, which are illustrated in Fig. 4.

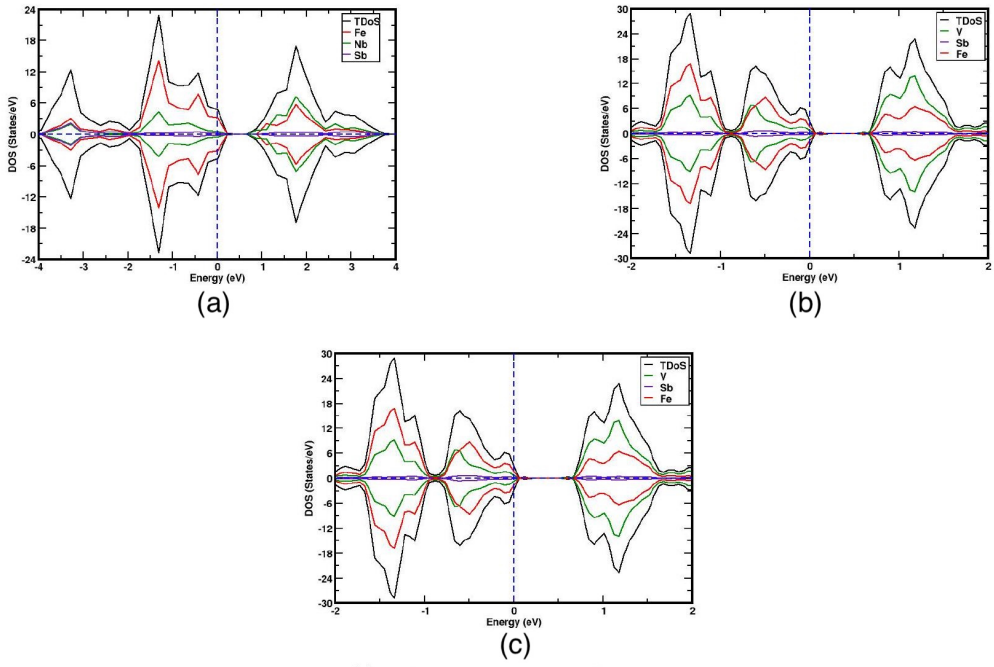

Figure 4. Density of states (DOS) plots of: (a) DOS of NbFeSb HH compound, (b) DOS of VFeSb HH compound, and (c) DOS of TaFeSb HH compound. The horizontal dotted line separates the up- and down-spin states of electrons in the atomic orbitals of the material, while the vertical dotted line distinguishes the electronic bands.

In Fig. 4, it is observed that spin-up and spin-down states of individual atoms in the NbFeSb, VFeSb, and TaFeSb, HH compounds are equally (symmetrically) distributed around the Fermi energy level. They indicate that the magnetic moment generated by the electronic spin states cancels out, and hence, the considered compounds exhibit non-magnetic properties. The nature of magnetic properties of

HH compounds is also predicted by the Slater-Pauling equation: $M = (Z - 18)\mu_B$ [67]. This equation is used to calculate the total magnetic moments of HH materials with a valence electron count (VEC) of 18. Each of the NbFeSb, VFeSb, and TaFeSb HH compounds has a VEC of 18, so the M of these compounds is equal to zero. Hence, they are non-magnetic materials. Thus, from the analysis of DOS and Slater-Pauling equation, the considered materials have non-magnetic characteristics.

The DOS illustrates the overall spin imbalance and magnetic characteristics of a material, whereas the PDOS determines the atomic and orbital sources of its magnetism [68]. The magnetism in materials often originates from partially filled p, d, or f orbitals. A significant difference between the spin-up and spin-down PDOS of these orbitals indicates the presence of localized magnetic moments. Additionally, orbital hybridization (e.g., d-orbitals of one atom with p-orbitals of neighboring atoms) affects exchange interactions, thereby influencing magnetic ordering. The PDOS plots of NbFeSb, VFeSb, and TaFeSb HH compounds are illustrated in Fig. 5.

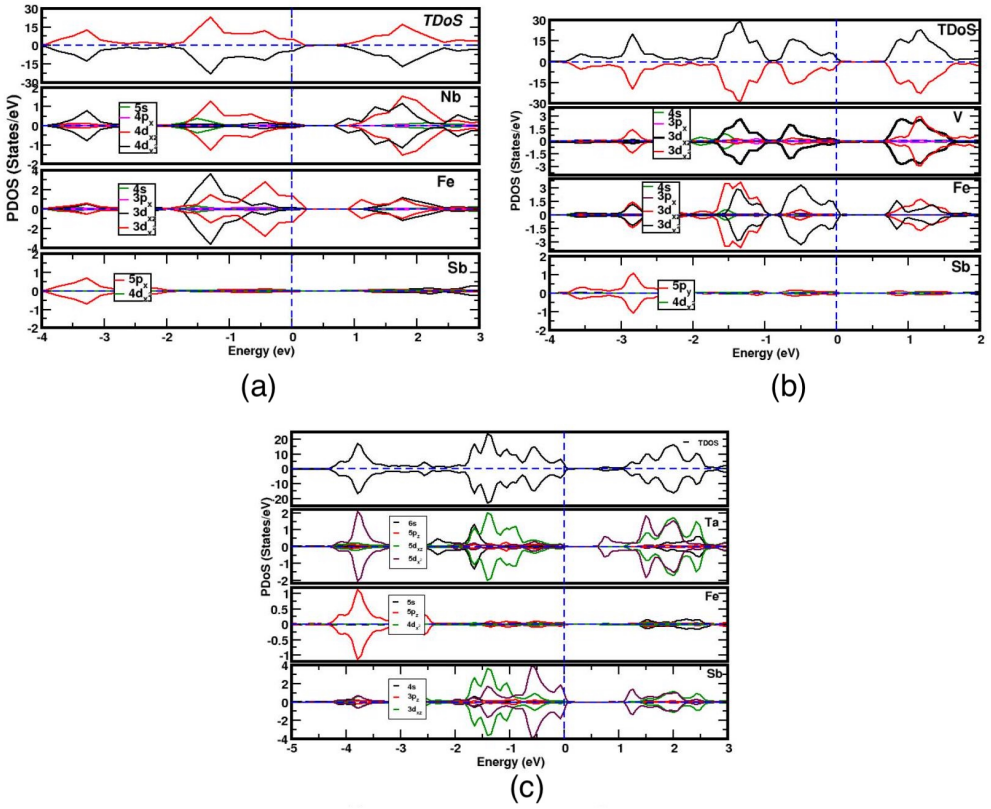

Figure 5. Partial density of states (PDOS) plots of; (a) PDOS of NbFeSb HH compound, (b) PDOS of VFeSb HH compound, (c) PDOS of TaFeSb HH compound. The horizontal dotted line separates the spin-up and spin-down states of electrons in the individual orbital of atoms present in the materials, while the vertical dotted line distinguishes the electronic bands.

We have calculated the magnetic moment and found that the spin-up states in the 5 s, $4p_x, 4d_{xz}, 4d_{x^2}$ orbitals of Nb atoms, 4 s, $3p_x, 3d_{xz}, 3d_{xz}$ orbitals of Fe atoms, and $5p_x, 4d_{x^2}$ orbitals of Sb atoms in the

NbFeSb compound have values equal to those of the corresponding down-spin states in the respective orbitals. The total magnetic moment is zero, as it results from the cancellation of the magnitudes of both spin states. Thus, NbFeSb is a non-magnetic material. Similarly, the magnetic moment of the VFeSb compound shows that the spin-up states in the 4 s, $3p_x, 3d_{xz}, 3d_{x^2}$ orbitals of V atoms; 4 s, $3p_x$, $3d_{xz}, 3d_{x^2}$ orbitals of Fe atoms; and $5p_x, 4d_{x^2}$ orbitals of Sb atoms have values equal to those of the corresponding down-spin states in the respective orbitals. The total magnetic moment is zero, resulting from the cancellation of the magnitudes of both spin states. Therefore, VFeSb is a non-magnetic material.

Moreover, we have computed the magnetic moment of the TaFeSb HH compound. The calculated magnetic moment of the TaFeSb compound shows that the spin-up states in the 6s, $5p_z, 5d_{xz}, 5d_{x^2}$ orbitals of Ta atoms; 4s, $3p_x, 3d_{xz}, 3d_{x^2}$ orbitals of Fe atoms; and $5p_x, 4d_{x^2}$ orbitals of Sb atoms have values equal to those of the corresponding down-spin states in the respective orbitals. The total magnetic moment is zero, due to the cancellation of the magnitudes of both spin states. Therefore, TaFeSb has non-magnetic properties. Based on the DOS and PDOS analysis of the NbFeSb, VFeSb, and TaFeSb HH compounds, we conclude that these materials exhibit non-magnetic properties. This calculation is consistent with previously reported results for the same compounds [37].

IV. Conclusions

We perform a theoretical analysis of NbFeSb, VFeSb, and TaFeSb materials by investigating their structural, mechanical, dynamical, thermal, electronic, and magnetic properties using the VASP computational code with the PBE functional. For the structural properties, we calculated the ground-state energy and the bond lengths between nearest-neighbor atoms in the materials. We found that the considered materials possess minimum ground state energies, indicating that they are structurally stable compounds. The bonding of atoms in the structures further confirms that the atoms are tightly bound to each other. The mechanical properties of the materials are examined through the calculations of their elastic constants and modulus of rigidity, and it is found that NbFeSb, VFeSb, and TaFeSb are mechanically stable. From the analysis of the modulus of rigidity, it is observed that they possess greater hardness. Based on the calculated value of the isotropic index, the considered materials exhibit an anisotropic nature. The ductility or brittleness of the materials is examined through the calculated values of Pugh's ratio and position's ratio, and it is found that NbFeSb and TaFeSb have ductile properties, whereas VFeSb exhibits a brittle nature. The dynamical properties of the materials are examined through the phonon dispersion curves, and it is found that all frequency curves possess positive values at each symmetric point, indicating that the considered materials are dynamically stable. The thermal properties of the materials are investigated by calculating their phonon velocities and Debye temperatures, and it is found that NbFeSb, VFeSb, and TaFeSb have good thermal properties. The electronic properties of

NbFeSb, VFeSb, and TaFeSb are explored through the analysis of their band structures and DOS plots, and the band gaps are found to be 0.80 eV, 0.70 eV, and 0.73 eV , respectively. Hence, they are small band-gap semiconducting materials. Moreover, the DOS and PDOS plots of the considered compounds show symmetrically distributed up- and down-spin states around the Fermi energy level. The resultant values of the magnetic moments of NbFeSb, VFeSb, and TaFeSb are found to be zero; hence, they exhibit non-magnetic properties.

V. Acknowledgements

The authors would like to thank the International Science Program (ISP), Uppsala University, Sweden, for supporting the Atmospheric and Material Science Research Group at the Department of physics, Amrit Campus, through NEP01 to conduct the computational work.

References

[1] Li G, Hao S, Aydemir U, Wood M, Goddard III WA, Zhai P, et al. Structure and failure mechanism of the thermoelectric CoSb3/TiCoSb interface. ACS Applied Materials & Interfaces. 2016;8(46):31968-77.

[2] Larson P, Mahanti SD, Kanatzidis MG. Structural stability of Ni-containing half-Heusler compounds. Physical Review B. 2000;62(19):12754-62.

[3] Ma J, et al. Computational investigation of half-Heusler compounds for spintronics applications. Physical Review B. 2017;95(2):024411.

[4] Alijani V, Winterlik J, Fecher GH, Naghavi SS, Felser C. Quaternary half-metallic Heusler ferromagnets for spintronics applications. Physical Review B. 2011;83(18):184428.

[5] Gruhn T. Comparative ab initio study of half-Heusler compounds for optoelectronic applications. Physical Review B. 2010;82(12):125210.

[6] Kieven D, Klenk R, Naghavi S, Felser C, Gruhn T. I-II-V half-Heusler compounds for optoelectronics: Ab initio calculations. Physical Review B. 2010;81(7):075208.

[7] Kojima T, Kameoka S, Tsai AP. The emergence of Heusler alloy catalysts. Science and Technology of Advanced Materials. 2019;20(1):445-55.

[8] Lee MS, Poudeu FP, Mahanti SD. Electronic structure and thermoelectric properties of Sb-based semiconducting half-Heusler compounds. Physical Review B. 2011;83(8):085204.

[9] Prinz GA. Magnetoelectronics applications. Journal of Magnetism and Magnetic Materials. 1999;200(1–3):57-68.

[10] Pan Y, et al. Superconductivity and magnetic order in the noncentrosymmetric half-Heusler com-

pound ErPdBi. Europhysics Letters. 2013;104(2):27001.

[11] Villars P. Pearson's Handbook: Crystallographic Data for Intermetallic Phases. vol. 1. ASM International; 1997.

[12] Graf T, Felser C, Parkin SS. Simple rules for the understanding of Heusler compounds. Progress in Solid State Chemistry. 2011;39(1):1-50.

[13] Zeier WG, et al. Engineering half-Heusler thermoelectric materials using Zintl chemistry. Nature Reviews Materials. 2016;1(6):1-10.

[14] Anand S, et al. A valence balanced rule for discovery of 18-electron half-Heuslers with defects. Energy & Environmental Science. 2018;11(6):1480-8.

[15] Pierre J, Skolozdra RV, Gorelenko YK, Kouacou M. From nonmagnetic semiconductor to itinerant ferromagnet in the TiNiSn-TiCoSn series. Journal of Magnetism and Magnetic Materials. 1994;134(1):95-105.

[16] Tobola J, Pierre J, Kaprzyk S, Skolozdra RV, Kouacou MA. Crossover from semiconductor to magnetic metal in semi-Heusler phases as a function of valence electron concentration. Journal of Physics: Condensed Matter. 1998;10(5):1013.

[17] Offernes L, Ravindran P, Kjekshus A. Electronic structure and chemical bonding in half-Heusler phases. Journal of Alloys and Compounds. 2007;439(1–2):37-54.

[18] Wijn HPJ. Alloys and compounds of 3d elements with main group elements. In: Magnetic Properties of Metals. Berlin, Heidelberg: Springer; 1991. p. 95-158.

[19] Aliev FG. Gap at Fermi level in some new d- and f-electron intermetallic compounds. Physica B: Condensed Matter. 1991;171(1–4):199-205.

[20] Nakajima Y, Hu R, Kirshenbaum K, Hughes A, Syers P, Wang X, et al. Superconductivity and magnetism in RPdBi compounds. Science Advances. 2015;1(5):e1500242.

[21] Eliassen S, Author2 B, Author3 C. Lattice thermal conductivity in (Ti, Zr, Hf)NiSn alloys. Journal of Applied Physics. 2017;121(17):175106.

[22] Kim H, Meinert M. High-throughput DFT discovery of new Half-Heusler compounds for thermoelectric applications. Physical Review Materials. 2018;2(12):123801.

[23] Mohamed MAA, Ibrahim EMM, Rodriguez NP, Hampel S, Buechner B, Schierning G, et al. Co-doping NbFeSb with Sn and Hf: Tuning electronic and phonon properties. Acta Materialia. 2020;196:669-76.

[24] Bouldiab K, Khenata A, Mengibar N, Bouhemadou S, Boulahya T, Sahnoun M. Structural, electronic, magnetic, and thermal properties of Half-Heusler compounds. Journal of Materials Science. 2021;56(20):11856-65.

[25] Lopes MC, Antonelli A. Pd-based Half-Heusler compounds: Electronic, vibrational, and defect properties. arXiv preprint arXiv:231209186. 2023.

[26] Lopes MC, Antonelli A. Ti-based Half-Heusler compounds: Electronic, vibrational, and defect properties. arXiv preprint arXiv:231209186. 2023.

[27] Kohn W, Sham L. Density functional theory. In: Conference Proceedings – Italian Physical Society. Editrice Compositori; 1996. p. 561-72.

[28] Hafner J. Ab-initio simulations of materials using VASP: Density-functional theory and beyond. Journal of Computational Chemistry. 2008;29(13):2044-78.

[29] Perdew JP, Burke K, Ernzerhof M. Generalized gradient approximation made simple. Physical Review Letters. 1996;77(18):3865-8.

[30] Di Ventra M, Pantelides ST. Hellmann–Feynman theorem and the definition of forces in quantum time-dependent and transport problems. Physical Review B. 2000;61(23):16207-10.

[31] Togo A, Tanaka I. First principles phonon calculations in materials science. Scripta Materialia. 2015;108:1-5.

[32] Körner W, Elsässer C. First-principles density functional study of dopant elements at grain boundaries in ZnO. Physical Review B. 2010;81(8):085324.

[33] Pines D, Bohm D. A collective description of electron interactions: II. Collective vs individual particle aspects of the interactions. Physical Review. 1952;85(2):338-53.

[34] Bohm D, Pines D. A collective description of electron interactions: III. Coulomb interactions in a degenerate electron gas. Physical Review. 1953;92(3):609-25.

[35] Evers CB, Richter CG, Hartjes K, Jeitschko W. Ternary transition metal antimonides and bismuthides with MgAgAs-type and filled NiAs-type structure. Journal of Alloys and Compounds. 1997;252(1–2):93-7.

[36] Li G, et al. Enhanced ideal strength of thermoelectric half-Heusler TiNiSn by sub-structure engineering. Journal of Materials Chemistry A. 2016;4(38):14625-36.

[37] Bencherif K. Optical and thermal properties of the half-Heusler VFeSb and NbFeSb alloys. Revista Mexicana de Física. 2022;68(2).

[38] Bilińska K, Winiarski MJ. High-throughput exploration of half-Heusler phases for thermoelectric applications. Crystals. 2023;13(9):1378.

[39] Voigt W. Üeber die Beziehung zwischen den beiden Elasticitätsconstanten isotroper Körper. Annalen der Physik. 1889;274(12):573-87.

[40] Reuß A. Berechnung der Fließgrenze von Mischkristallen auf Grund der Plastizitätsbedingung für Einkristalle. Zeitschrift für Angewandte Mathematik und Mechanik. 1929;9(1):49-58.

[41] Hill R. The elastic behaviour of a crystalline aggregate. Proceedings of the Physical Society Section A. 1952;65(5):349-54.

[42] Born M, Fürth R. The stability of crystal lattices. III: An attempt to calculate the tensile strength of a cubic lattice by purely static considerations. In: Mathematical Proceedings of the Cambridge

Philosophical Society. vol. 36; 1940. p. 454-65.

[43] Pugh SF. XCI. Philosophical Magazine. 1954;45:823-44.

[44] Ali MA, Hadi MA, Hossain MM, Naqib SH, Islam AKMA. Theoretical investigation of structural, elastic, and electronic properties of ternary boride MoAlB. Physica Status Solidi B. 2017;254(7):170017.

[45] Shulumba N. Vibrations in solids from first principles: Lattice dynamics to high temperature phase stability. Sweden: Linköpings Universitet; 2015.

[46] Neupane HK, Oli D, Rijal OS, Neupane RK, Shrestha P, Sharma S, et al. Exploring the structural, dynamical, mechanical, electronic, magnetic, and optical properties of Ta_2AlN, Ti_2AlN & Ti_2GaN MAX phase compounds: First-principles study. Heliyon. 2025;11(6).

[47] Neupane HK, Rijal OS, Neupane RK, Paudel G, Shrestha P, Sharma S, et al. Structural, dynamical, thermomechanical, electronic, magnetic, and optical properties of M_2AC (M = Ta, Sc; A = Al, Cd) MAX phase compound via DFT approach. Physica Scripta. 2025;100:095921.

[48] Pokharel A, Khanal K, Yadav SK, Neupane T, Paudel G, Rijal OS, et al. Exploring the structural, electronic, and magnetic properties of $MoTe_2$ and $MoSe_2$ materials via DFT+U approach. Journal of the Nepal Chemical Society. 2025;45(2):11-24.

[49] Çoban C, Çolakoğlu K, Çiftçi YÖ. First principles study of the structural, mechanical, phonon, optical, and thermodynamic properties of half-Heusler (HH) compound NbFeSb. Physica Scripta. 2015;90(9):095701.

[50] Rached Y, Ait Belkacem AA, Rached D, Rached H, Caid M, Merabet M, et al. The stability and electronic and thermal transport properties of new Tl-based MAX-phase compound Ta_2TlX (X = C or N). Physica Status Solidi B. 2022;259(11):2200195.

[51] Long Y, Chen J. Theoretical study of the phonon–phonon scattering mechanism and the thermal conductive coefficients for energetic material. Philosophical Magazine. 2017;97(28):2575-95.

[52] Wang Y, Lu Z, Ruan X. First principles calculation of lattice thermal conductivity of metals considering phonon–phonon and phonon–electron scattering. Journal of Applied Physics. 2016;119(22):225101.

[53] Barsoum MW, Radovic M. Elastic and mechanical properties of the MAX phases. Annual Review of Materials Research. 2011;41(1):195-227.

[54] Sun Z, Li S, Ahuja R, Schneider JM. Study of MAX-phase-related properties. Solid State Communications. 2004;129:589-93.

[55] Dar SA. A unified DFT understanding on electronic, magnetic, elastic, mechanical, thermodynamic, and thermoelectric results of Ru_2MnV and Ru_2MnNb full Heusler alloy; 2025. Unpublished manuscript.

[56] Hummel RE. Electronic Properties of Materials. New York: Springer Science & Business Media;

2011.

[57] Neupane HK, Adhikari NP. Structure, electronic and magnetic properties of 2D graphene–molybdenum disulphide (G–MoS_2) heterostructure with vacancy defects at Mo sites. Computational Condensed Matter. 2020;24:e00489.

[58] Paudel G, Nepal M, Aryal S, Devkota A, Neupane HK. Effect of water adsorption on bilayer h-BN: First-principles study. Journal of Nepal Physical Society. 2023;9(2):56-62.

[59] Neupane HK, Adhikari NP. Structural, electronic and magnetic properties of impurity-defected graphene/MoS_2 van der Waals heterostructure: First-principles study. Journal of Nepal Physical Society. 2021;7(2):1-8.

[60] Rahman MA. A review on semiconductors including applications and temperature effects in semiconductors. American Scientific Research Journal for Engineering, Technology, and Sciences. 2014;7(1):50-70.

[61] Proceedings of the Physical Society. vol. 36. Institute of Physics and the Physical Society.; 1924.

[62] Aryal S, Paudel G, Nepal M, Oli D, Rijal OS, Neupane HK. Water adsorption on pristine and vacancy-defected h-BN monolayer: First-principles study. Journal of Institute of Science and Technology. 2025;30(1):73-81.

[63] Lawati DR, Neupane HK, Chaudhary DK, Shrestha P, Adhikari RP, Joshi LP, et al. Structural, mechanical, electronic and optical properties of $MgZnO_3$ perovskite: First-principles study. Journal of Physics and Chemistry of Solids. 2023;181:111547.

[64] Nepal M, Paudel G, Aryal S, Devkota A, Neupane HK. Adsorption of water on vacancy-defective h-BN bilayer at B and N sites: First-principles calculation. Bibechana. 2024;21(2):129-41.

[65] Neupane HK, Adhikari NP. First-principles study of defected single-layer hexagonal boron nitride (h-BN). Nepal Journal of Science and Technology. 2021;20(2):55-66.

[66] Rijal OS, Neupane HK, Oli D, Neupane RK, Shrestha P, Sharma S, et al. A first-principles investigation of the structural, mechanical, dynamic, electronic, magnetic, and optical properties of Ti_2AC (A = Cd, S) MAX phase compounds. Journal of Physics D: Applied Physics. 2025;58(12):125102.

[67] Slatter L, Lim WYS, Zhang D, Duran SSF, Tan XY, Tan CKI, et al. Physical intuition to improve electronic properties of thermoelectrics. Frontiers in Physics. 2021;9:755597.

[68] Rafiq Q, Hayat SS, Azam S. First-principles calculations to investigate electronic, magnetic, and optical properties at (110) and (111) surfaces of Ni adsorption on CdO. Molecular Physics. 2024;122(24):e2341117.